

# MWCNT interactions with protein: surface-induced changes in protein adsorption and the impact of protein corona on cellular uptake and cytotoxicity

This article was published in the following Dove Medical Press journal:  
*International Journal of Nanomedicine*

Ting Zhang<sup>1,2</sup>  
Meng Tang<sup>1,2</sup>  
Ying Yao<sup>1</sup>  
Ying Ma<sup>1</sup>  
Yuepu Pu<sup>1,2</sup>

<sup>1</sup>Key Laboratory of Environmental Medicine and Engineering, Ministry of Education, Department of Occupational and Environmental Health, School of Public Health & Collaborative Innovation Center of Suzhou Nano Science and Technology Southeast University, Nanjing, Jiangsu, 210009, China; <sup>2</sup>Jiangsu Key Laboratory for Biomaterials and Devices, Southeast University, Nanjing, Jiangsu, 210009, China

**Purpose:** Protein adsorption onto nanoparticles in the form of protein corona, affects properties of nanomaterials and their behavior in the biological milieu. This study aims at exploring the effects of multiwalled carbon nanotubes (MWCNTs) surface chemistry on bovine serum albumin (BSA) and immunoglobulin G (IgG), including their adsorption behavior and spatial configurations, as well as the impact on cellular uptake, cytotoxicity, and cellular responses.

**Methods:** Three types of MWCNTs (pristine MWCNTs, MWCNTs-COOH, and MWCNTs-PEG) were synthesized by classical chemical reduction. The size, morphology, hydrodynamic size, and zeta potential were characterized using transmission electron microscopy and dynamic light scattering. MWCNTs were exposed to BSA and IgG solutions, then the amount of MWCNT absorption was performed by bicinchoninic acid assay, and the effects were assessed by utilizing fluorescence spectroscopy, circular dichroism (CD) spectroscopy. Quantitative measurement of MWCNTs uptake with or without protein corona was performed as turbidity method. CCK assay and a microdilution method were performed to evaluate the effects of protein corona on cytotoxicity and pro-inflammatory cytokines release.

**Results:** The BSA and IgG adsorption capacities of MWCNTs followed the order pristine MWCNTs > MWCNTs-COOH and MWCNTs-PEG. MWCNT binding can cause fluorescence quenching and conformational changes in BSA and IgG, indicating that both the physicochemical properties of MWCNTs and protein properties play critical roles in determining their adsorption behavior. Further study showed time-dependent increases in MWCNT cellular uptake and internalization. Hydrophobicity is the major factor increasing cellular uptake of pristine MWCNTs, but a protein corona enriched with dysoposins is the main factor reducing uptake of MWCNT-COOH by RAW264.7 cells. The cytotoxicity and pro-inflammatory response related to physicochemical properties of MWCNTs, and frustrated phagocytosis is a key initiating event in the pro-inflammatory response of MWCNT-exposed macrophages.

**Conclusion:** These findings shed light on how functionalized MWCNTs interact with protein coronas and provide useful insight into the dramatic effect of protein coronas on different functionalized MWCNTs. These events affect cellular uptake and cytotoxicity, which could inform how to enhance MWCNT biocompatibility and develop approaches for managing MWCNT hazards.

**Keywords:** multiwalled carbon nanotubes, protein corona, cellular uptake, cytotoxicity, inflammation

Correspondence: Ting Zhang  
Key Laboratory of Environmental Medicine Engineering, Ministry of Education, Department of Occupational and Environmental Health, School of Public Health, Southeast University, No. 87 Dingjiaqiao, Nanjing, Jiangsu 210009, China  
Tel +86 25 8327 2566  
Fax +86 25 8327 2564  
Email zhangting@seu.edu.cn

## Introduction

Multiwalled carbon nanotubes (MWCNTs) have unique structural, chemical, optical, and electronic properties that make them potential candidates for numerous applications

in biomedical fields.<sup>1</sup> Most investigations related to the toxicity of carbon nanotubes (CNTs) have focused on target organs, potential negative effects, cytotoxicity, and toxicity mechanisms.<sup>2</sup> Previous studies have already shown that MWCNTs inhibit cell proliferation and induce oxidative damage, apoptosis, or necrosis *in vitro*.<sup>3–7</sup> Inhalation of MWCNTs leads to pulmonary damage or systemic inflammatory reaction, oxidative damage, and genotoxicity.<sup>8</sup> However, few researchers have examined the interactions of CNTs with biological macromolecules. Most proteins are involved in life processes, and CNTs bound to proteins in systemic circulation are deposited in target organs through blood transport, where they can exert therapeutic or potential toxic effects.<sup>9–11</sup> In-depth exploration of interactions between CNTs and protein is important with regard to drug delivery applications and biological safety issues of CNTs. However, research in this area is still limited.

Plasma proteins tend to associate with the surface of nanoparticles (NPs), thus forming the so-called “protein corona.” Most investigations have been on protein adsorption to the surface of MWCNTs, binding locations, and protein conformational changes. A few investigations considered the further effects of protein conformational changes and cell damage. Conformational changes may lead to loss of protein activity and alter the surface properties of MWCNTs, including surface groups and charge, which may impact bioactivity. Furthermore, protein corona formation is highly dependent on the physicochemical properties of NPs. Pristine MWCNTs are highly hydrophobic due to the delocalization of  $\pi$ -electrons. Surface functionalization has been developed to improve their dispersion, stability, and biocompatibility by introducing carboxylic groups or other oxygen-containing groups. However, the possible impacts of MWCNT interactions with protein corona and subsequent influence on protein binding and biological responses have not been well described.

Our previous studies demonstrated that MWCNTs generate oxidative stress and pro-inflammatory responses in macrophages.<sup>12,13</sup> Furthermore, we reported *in vivo* exposure to pristine MWCNTs that caused systemic immunosuppression through splenic dysregulation.<sup>14</sup> Less attention has been paid to the impact of CNTs on immune-related proteins. Serum albumin and immunoglobulins are two important proteins involved in the immune response. BSA serves as a transportation or carrier protein in the body and plays a pivotal role in regulating the physiological balance of the blood. For these reasons, BSA is commonly used in *in vitro* models of the protein corona on NPs including carbon-based NPs.<sup>10</sup> The most abundant class of immunoglobulins in the blood is immunoglobulin G (IgG), which plays an indispensable role in the primary antibacterial immune response and humoral immune response. The

properties of change due to absorption of protein corona, which in turn alters NP surface properties and modulates biological behaviors including distribution, cellular uptake, and toxicity. The precise mechanisms underlying interactions between different types of MWCNTs and immune-related proteins and subsequent biological responses are still unclear.

In this study, we used pristine MWCNTs, carboxylated MWCNTs (MWCNTs-COOH), and polyethylene glycol MWCNTs (MWCNTs-PEG) to study protein adsorption behavior and spatial configurations of BSA and IgG. We investigated their subsequent effect on intracellular uptake and cytotoxicity, including cell viability, lactate dehydrogenase (LDH) leakage, and secretion of inflammatory factors. Finally, we explored the impact of phagocytosis on cytotoxicity and inflammatory cytokine production in response to protein-coating MWCNTs. Our results clarify the adsorption processes of BSA and IgG onto different MWCNT surfaces and the underlying mechanisms of the biological response to MWCNTs. These findings provide insight for enhancing MWCNT biocompatibility and could guide the development of approaches to manage MWCNT hazards.

## Materials and methods

### MWCNT preparation

Pristine MWCNTs (average diameter 10–20 nm, length 5–15  $\mu\text{m}$ , purity  $\geq 95\%$ ) were purchased from Shenzhen Nano Harbor Co. (Shenzhen, People’s Republic of China). The synthesis and characterization of MWCNTs (pristine MWCNTs, MWCNTs-COOH, and MWCNTs-PEG) were performed using procedures in which the three types of MWCNTs were synthesized in two steps (Figure 1A) as described in previous studies (see details in the Supplementary materials). For the experiments, three types of MWCNTs were weighed on an analytical balance and suspended in a solution of distilled (DI) water and BSA (Nanjing Sunshine Biotechnology Co., Ltd, Nanjing, People’s Republic of China) and IgG (Sigma Aldrich Co., St Louis, MO, USA). These suspensions were sonicated at 100 W output with a frequency of 42 kHz for 30 minutes in a water sonicator. The MWCNTs suspensions were characterized using transmission electron microscopy (TEM), dynamic light scattering (DLS) and zeta potential measurements (Zetasizer Nano ZS90, Malvern Instruments, Malvern, UK).

### Adsorption experiments

Two milligrams of BSA or IgG were dissolved in 10 mL PBS for a concentration of 0.2 mg/mL. For the experiments, samples (pristine MWCNTs, MWCNTs-COOH, and MWCNTs-PEG) were diluted to 0.5 mg/mL with those two protein solutions. First, the compound was incubated for different

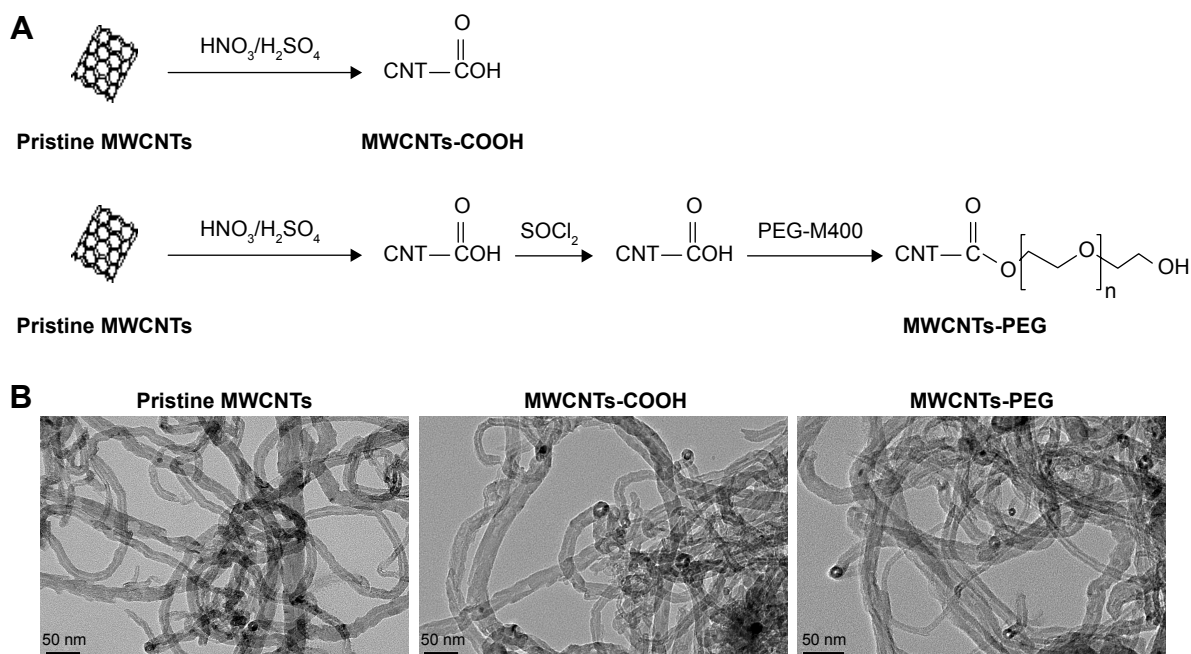


**Figure 1** Molecular structure and TEM images of MWCNTs.

**Notes:** (A) Schematic diagram showing functionalization of MWCNTs (B) TEM of three types of MWCNTs.

**Abbreviations:** MWCNTs, multiwalled carbon nanotubes; MWCNTs-COOH, carboxylated MWCNTs; MWCNTs-PEG, polyethylene glycol MWCNTs; TEM, transmission electron microscopy.

times (15 minutes, 30 minutes, 45 minutes, 1 hour, 2 hours, and 3 hours), and the supernatant was collected to measure unbound proteins using the bicinchoninic acid protein test (Beyotime Biotechnology, Jiangsu, People's Republic of China). The amount of MWCNT absorption was calculated and transformed as follows:  $m_{\text{absorption}} = (c_{\text{starting solution}} - c_{\text{supernatant}}) / m_{\text{MWCNTs}}$ . The T fluorescence spectra of native BSA, native IgG, and a protein solution of MWCNTs (pristine MWCNTs, MWCNTs-COOH, and MWCNTs-PEG) were recorded with an FL4600 spectrofluorometer (Hitachi, Tokyo, Japan) in a 1-cm quartz cuvette. The excitation wavelength was selected at 278 nm, and emission was monitored between 280 and 700 nm. The width of the excitation and emission slits was 5 nm, and the scan rate was 1,200 nm/min. The circular T spectra of proteins were recorded by using the Chirascan Spectropolarimeter (Applied Photophysics Ltd, Leatherhead, UK) in a 1-cm quartz cuvette. The detection wavelength range was between 190 and 280 nm. The wavelength slit width ( $\Delta\lambda=1$  nm), scan speed (100 nm/min), resolution (0.1 nm), and step distance (0.8 nm) were kept constant for all, and  $t$ , and the percentages of  $\alpha$ -helix,  $\beta$ -sheet (total of anti-parallel and parallel),  $\beta$ -turn, and random coil structures were analyzed using Chirascan software (Applied Photophysics Ltd).

## Cell culture and treatment

The murine macrophage cell line RAW264.7 was obtained from the American Type Culture Collection (Manassas, VA,

USA) and maintained in high glucose Dulbecco's minimum essential medium (DMEM) with 10% FBS at 37°C and 5% CO<sub>2</sub>. RAW264.7 cells were seeded in 96-well plates at a density of 5×10<sup>4</sup> cells/mL or 12-well plates at a density of 2×10<sup>5</sup> cells/mL for adherence overnight prior to treatment.

## Cellular uptake of MWCNTs

Changes in cellular uptake of MWCNTs with or without BSA and IgG coating were performed as our previous study described.<sup>12</sup> Briefly, MWCNTs were diluted with cell lysis solution followed by measuring the OD at 640 nm to quantify the MWCNTs. Cells were exposed to 25 μg/mL MWCNTs with and without BSA and IgG coating in serum-free medium (DMEM) for 2, 4, 6, 8, 12, or 24 hours, then cells were washed with PBS and lysed with 0.4 mL of 0.2 mol/L NaOH solution for 3 hours. Dimethyl sulfoxide (0.2 mL) was added to the lysate until MWCNTs were well dispersed in the lysate. A 250-μL sample was transferred to a 96-well plate, and the OD at 640 nm was measured.

## Cytotoxicities of the three types of MWCNTs

The influence of protein adsorption on the cytotoxicities of the three types of MWCNTs was examined by using WST-8 (Keygen Biotech Company, Nanjing, People's Republic of China), and LDH (Jiancheng Bioengineering, Nanjing, People's Republic of China) assays. RAW264.7 cells were exposed to

three types of MWCNTs with or without BSA and IgG coating at different concentrations (0, 25, 50, and 100  $\mu\text{g}/\text{mL}$ ) in serum-free culture conditions. After 24-hour incubation, WST-8 and LDH assays were used to determine cytotoxicities of the same treatment sample with viability assayed directly on cells and membrane integrity assayed by LDH release into the culture medium. The WST-8 and LDH assays were performed as previously described.<sup>15</sup> In addition, to assess cell morphology changes after MWCNTs exposure, RAW264.7 cells were incubated with 25  $\mu\text{g}/\text{mL}$  of MWCNTs in FBS-free or 10% FBS medium for 6 hours and washed with PBS twice, and then were fixed for 10 minutes with 4% paraformaldehyde at room temperature. The cells were observed under an Olympus IX50 inverted microscope (Olympus, Tokyo, Japan).

### Determination of pro-inflammatory cytokines in RAW264.7 cells stimulated by MWCNTs

To evaluate the effect of protein adsorption on inflammatory cytokine production, interleukin (IL)-1 $\beta$  and tumor necrosis factor (TNF)- $\alpha$  concentrations in the culture medium were determined using the “Ready-Set-Go” kit from (eBioscience, San Diego, CA, USA). RAW264.7 cells were exposed to MWCNTs with or without BSA and IgG coating at two different concentrations (25 and 100  $\mu\text{g}/\text{mL}$ ) for 24 hours in serum-free culture conditions.

### Assessment of the role of phagocytosis on cytotoxicity and inflammatory cytokine production of BSA-coated MWCNTs

To evaluate the role of phagocytosis on cytotoxicity and pro-inflammatory cytokine production in response to coated and uncoated MWCNTs, Cytochalasin D (CytoD, C8273, Sigma-Aldrich Co.) was used to inhibit phagocytosis.

MWCNT-only treated cells were used as controls and compared with inhibitor plus MWCNT-treated cells. Briefly, cells were preincubated for with 4  $\mu\text{M}$  CytoD for 2 hours prior to incubation with MWCNTs with or without BSA corona. Changes in MWCNT cellular uptake with or without CytoD were assessed by the standard turbidimetric method after 6 hours of MWCNT (25  $\mu\text{g}/\text{mL}$ ) incubation, cytotoxicity was evaluated by WST-8 and LDH assays, and IL-1 $\beta$  was measured by enzyme-linked immunosorbent assay (ELISA) after 24 hours of MWCNT (100  $\mu\text{g}/\text{mL}$ ) incubation. All the methods were completed using the procedures described above.

### Statistical analyses

All experiments were repeated at least three times. All data are expressed as mean  $\pm$  SD for the indicated number of independently performed experiments. Statistical analysis was performed using Student's *t*-test, and  $P < 0.05$  was considered statistically significant.

## Results

### Characterization of protein-crowned MWCNTs

The characterization of MWCNTs (pristine MWCNTs, MWCNTs-COOH, and MWCNTs-PEG) was performed using previously described procedures (see details in the Supplementary materials). TEM analysis in water revealed long ropes of bundled MWCNTs (Figure 1B). To assess the impact of the protein corona on MWCNT size, hydrodynamic size, and surface charge, the samples were dispersed in three types of media: DI water ( $\text{H}_2\text{O}$ ), 0.2 mg/mL BSA, and IgG solution. The corresponding hydrodynamic diameters of these three MWCNT medium dispersions were measured using DLS as shown in Table 1. Compared to the large hydrodynamic size of pristine MWCNTs in  $\text{H}_2\text{O}$  (523.7 nm), BSA-adsorbed

**Table 1** Characterization of MWCNTs

	Pristine MWCNTs	MWCNTs-COOH	MWCNTs-PEG
Diameter (nm)	10–20	10–20	10–20
Length ( $\mu\text{m}$ )	5–15	0.3–0.6	0.3–0.6
Zeta potential (mV)			
In $\text{H}_2\text{O}$	–14.97	–31.93	–15.60
In $\text{H}_2\text{O}$ (BSA-dispersed)	–15.83	–13.90	–19.03
In $\text{H}_2\text{O}$ (IgG-dispersed)	–13.83	–11.72	–17.21
Hydrodynamic size by DLS (nm)			
In $\text{H}_2\text{O}$	523.7	116.50	87.13
In $\text{H}_2\text{O}$ (BSA-dispersed)	320.27	108.40	87.10
In $\text{H}_2\text{O}$ (IgG-dispersed)	287.32	102.59	86.91

**Abbreviations:** DLS, dynamic light scattering; IgG, immunoglobulin G; MWCNTs, multiwalled carbon nanotubes; MWCNTs-COOH, carboxylated MWCNTs; MWCNTs-PEG, polyethylene glycol MWCNTs.

and IgG-adsorbed pristine MWCNTs showed a 34%–45% decrease in hydrodynamic size (287–340 nm), but BSA and IgG binding had no significant effect on the hydrodynamic sizes of MWCNTs-COOH or MWCNTs-PEG. The zeta potentials of all MWCNTs were negatively charged in water and protein medium. It is worth noting that the zeta potential of MWCNTs-COOH at H<sub>2</sub>O was –31.93 mV, while those for BSA and IgG were –15.90 mV and –11.72 mV, respectively.

## Qualitative assessment of BSA and IgG adsorption by MWCNTs

To evaluate interactions between MWCNTs and protein solutions after simple mixing, we explored the adsorption kinetics at different time points as shown in Figure 2A. The adsorption process was rapid in the initial stages (0–15 minutes) and the binding of BSA and IgG to MWCNTs reached equilibrium within 45 minutes. The results showed that a large amount of protein had adsorbed the surfaces of nanosheets, and the adsorption capacities of BSA and IgG followed an

order: pristine MWCNTs > MWCNTs-COOH > MWCNTs-PEG. The adsorption rate of pristine MWCNTs to BSA and IgG is between 30% and 45%, that of MWCNTs-COOH is between 5% and 15%, and the adsorption rate of MWCNTs-PEG is the lowest at ~5%.

## Fluorescence spectra analysis of protein corona

To obtain structural information at the tertiary level, the intrinsic tryptophan fluorescence of BSA and IgG in the presence of different types of MWCNTs or alone was measured. As shown in Figure 2B, BSA exhibited a strong fluorescence emission peak at 339 nm on excitation. After proteins adsorbed on the MWCNT surface, the fluorescence intensity of tryptophan residues was quenched by different types of MWCNTs, and the fluorescence intensity of BSA and IgG followed the order native BSA/IgG > MWCNTs-PEG > MWCNTs-COOH > pristine MWCNTs. A blue shift was measured in the presence of –COOH and pristine MWCNTs.

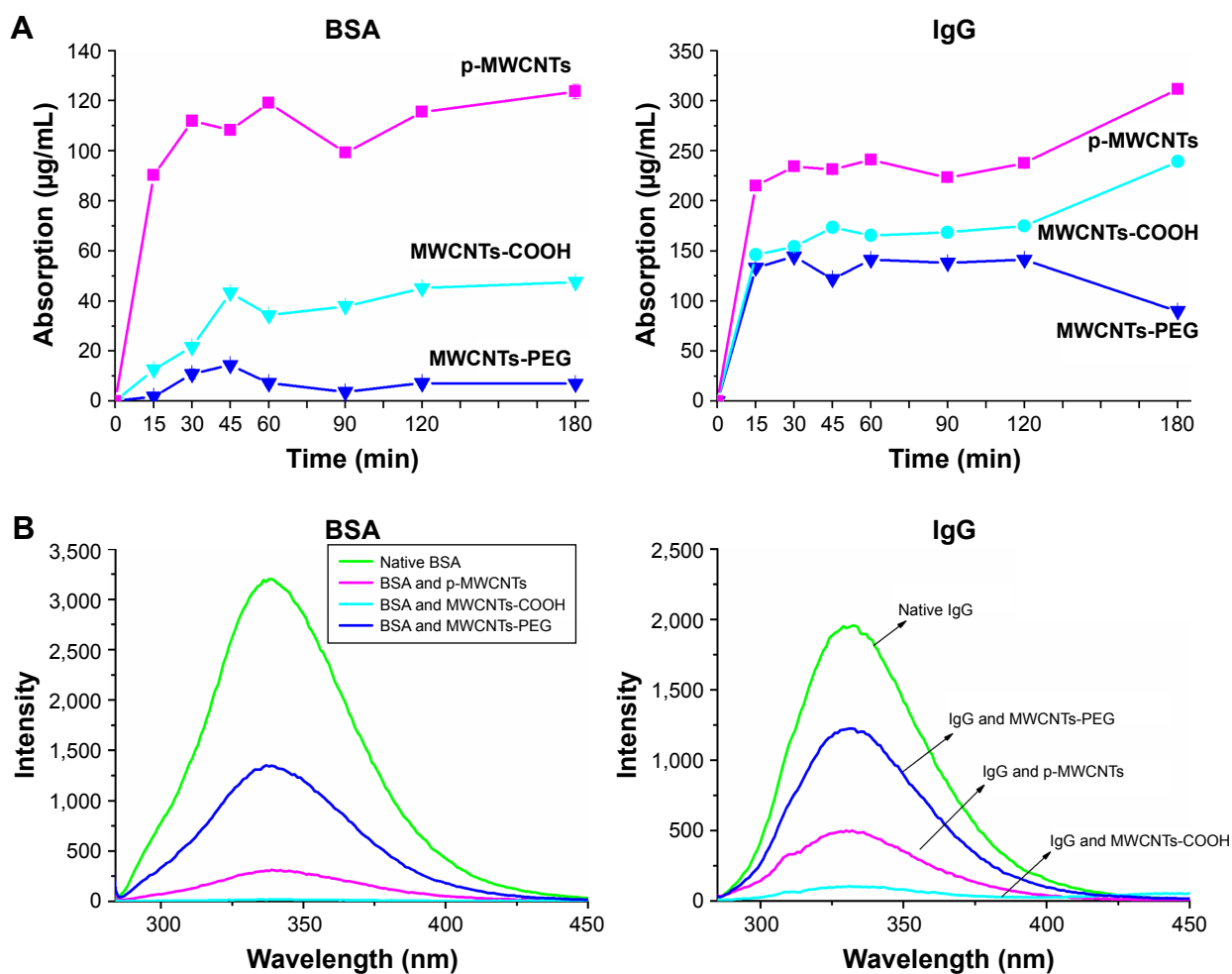
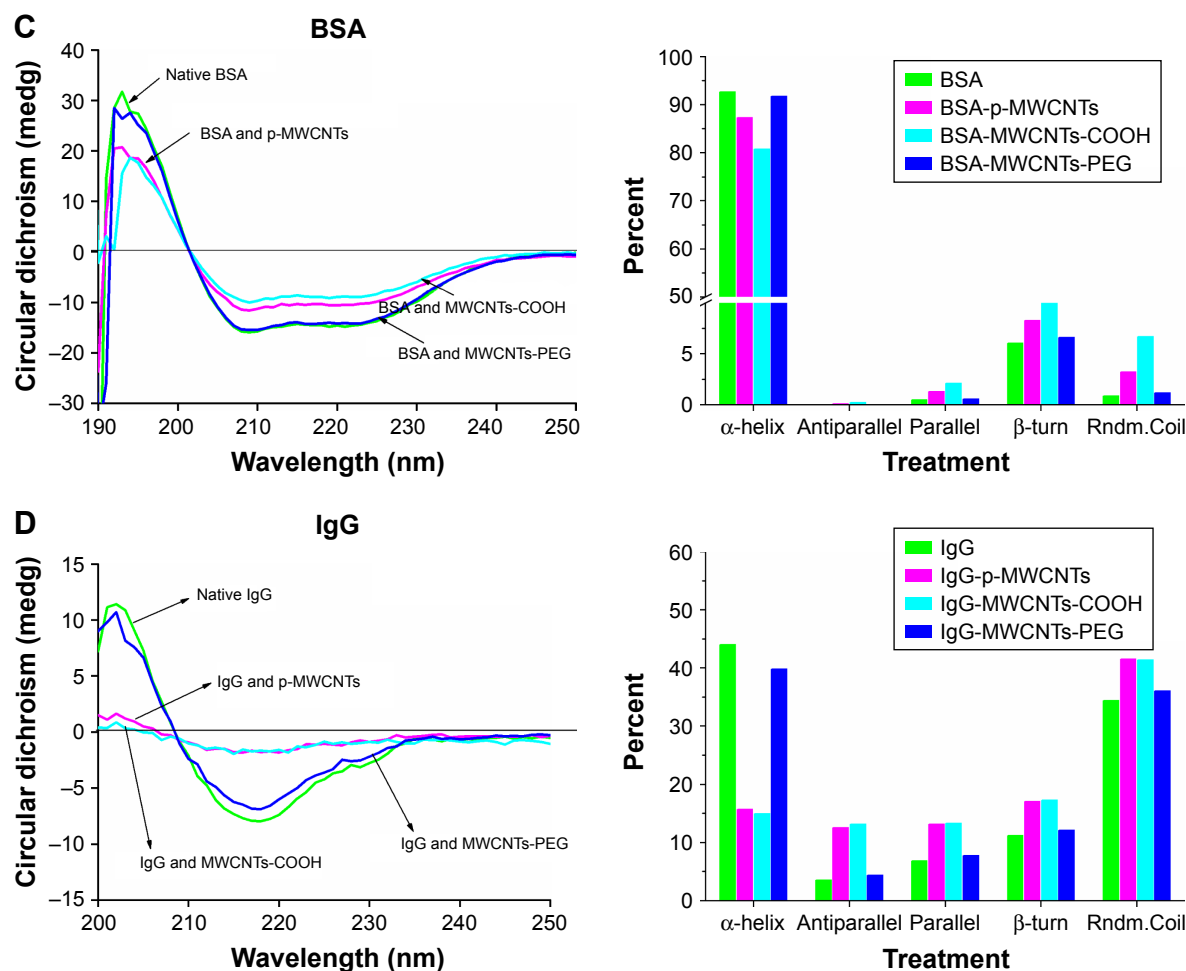


Figure 2 (Continued)



**Figure 2** The binding interaction of MWCNTs with BSA and IgG.

**Notes:** (A) Quantification of BSA (left) and IgG (right) bound to MWCNTs using BCA protein assay. (B) Fluorescence emission spectra of BSA (left) and IgG (right) in the absence and presence of three types of MWCNTs. MWCNTs were dispersed in BSA or IgG solution (0.2 mg/mL) at 25°C for 60 minutes, then the solution was tested by emission spectra at an excitation wavelength of 278 nm. Circular dichroism spectra of BSA (C) and IgG (D) in the absence and presence of three types of MWCNTs. MWCNTs were dispersed in BSA solution (0.2 mg/mL) at 25°C for 60 minutes, and then the solution was tested by circular dichroism spectra (left) at 190–280 nm. Percent of secondary (right) BSA and IgG structures inferred from the CD spectra.

**Abbreviations:** BCA, bicinchoninic acid; IgG, immunoglobulin G; MWCNTs, multiwalled carbon nanotubes; MWCNTs-COOH, carboxylated MWCNTs; MWCNTs-PEG, polyethylene glycol MWCNTs.

## CD analysis for secondary structure changes of protein coronas

The effect of MWCNTs on adsorbed protein conformation was assessed using CD spectroscopy. As shown in Figure 2C, the CD spectrum of BSA exhibited two negative bands at 208 and 222 nm, which is the characteristic feature of  $\alpha$ -helix structure. After the proteins adsorbed on MWCNT surfaces, the CD spectra of BSA progressively shifted to lower ellipticity values around 208 and 220 nm in the presence of pristine MWCNTs and MWCNTs-COOH; however, incubation with MWCNTs-PEG did not dramatically affect the CD spectrum. The relative contribution of each secondary structural element was calculated as shown in the right panel of Figure 2C. The  $\alpha$ -helicity was at 208 nm, while  $\alpha$ -helicity

of BSA alone was 93%. For BSA in the presence of the pristine MWCNTs and MWCNTs-COOH, the respective alpha-helicity values were 87% and 81%. For MWCNTs-PEG, there was almost no change in  $\alpha$ -helicity. CD results of BSA also showed slight increases of antiparallel, parallel,  $\beta$ -turn, and random coil on pristine MWCNTs and MWCNTs-COOH. Similar results were observed for IgG in the presence of different types of MWCNTs (Figure 2D). For IgG, incubation with MWCNTs led to a significant reduction in the negative ellipticity around 210–235 nm, which indicates destruction of  $\alpha$ -helical structures. The CD results of IgG also showed a significant decrease of  $\alpha$ -helicity and slight increases of antiparallel, parallel,  $\beta$ -turn, and random coil on pristine MWCNTs and MWCNTs-COOH,

but MWCNTs-PEG showed little change (Figure 2D). These results suggested that the interaction of pristine MWCNTs and MWCNTs-COOH with BSA and IgG led to loosening and unfolding of the protein skeleton.

### Intracellular uptake of MWCNTs-protein corona

To assess the effects of protein adsorption on cellular uptake of different types MWCNTs and the capability of MWCNT internalization, we investigated cellular association and uptake of BSA- and IgG-coronated MWCNTs and bare MWCNTs in macrophage RAW264.7 cells under FBS-free culture conditions (Figure 3). The results showed a time-dependent increase in uptake for MWCNTs with or without protein coronas. Quantitative assessment of uptake by RAW264.7 cells in serum-free DMEM suggested that significantly more protein corona pristine MWCNTs were internalized compared to bare pristine MWCNTs, whereas corona MWCNTs-COOH seemed to have lower levels of uptake than bare MWCNTs-COOH. The presence of protein corona had little effect on RAW264.7 uptake of MWCNTs-PEG.

### Cytotoxic effects of MWCNTs-protein corona

Dose-dependent decreases in cell viability after treatment with the three types of MWCNTs are shown in the left panels of Figure 4A and B. At the same dose, there was a significant decrease in viability of cells exposed to bare pristine MWCNTs and MWCNTs-COOH compared to that in cells treated with BSA-coronated MWCNTs, but protein corona did not have a significant effect on cell viability in the MWCNTs-PEG condition. The effect of IgG on the cytotoxicity of MWCNTs had a similar order to MWCNT binding capacity, and there was a significant decrease in cell viability of pristine MWCNTs and MWCNTs-COOH by adsorption of IgG, indicating more protein adsorbed led to a smaller cell viability decrease. Moreover, MWCNTs induced a dose-dependent release of LDH after 24 hours (right panels of Figure 4A and B). At the same dose, MWCNTs-COOH with or without protein corona released a higher amount of LDH, although this was reduced in protein-coronated MWCNTs-COOH; a significant effect was only observed for the highest concentration. However, pristine MWCNTs caused significant cell membrane damage compared to BSA- and

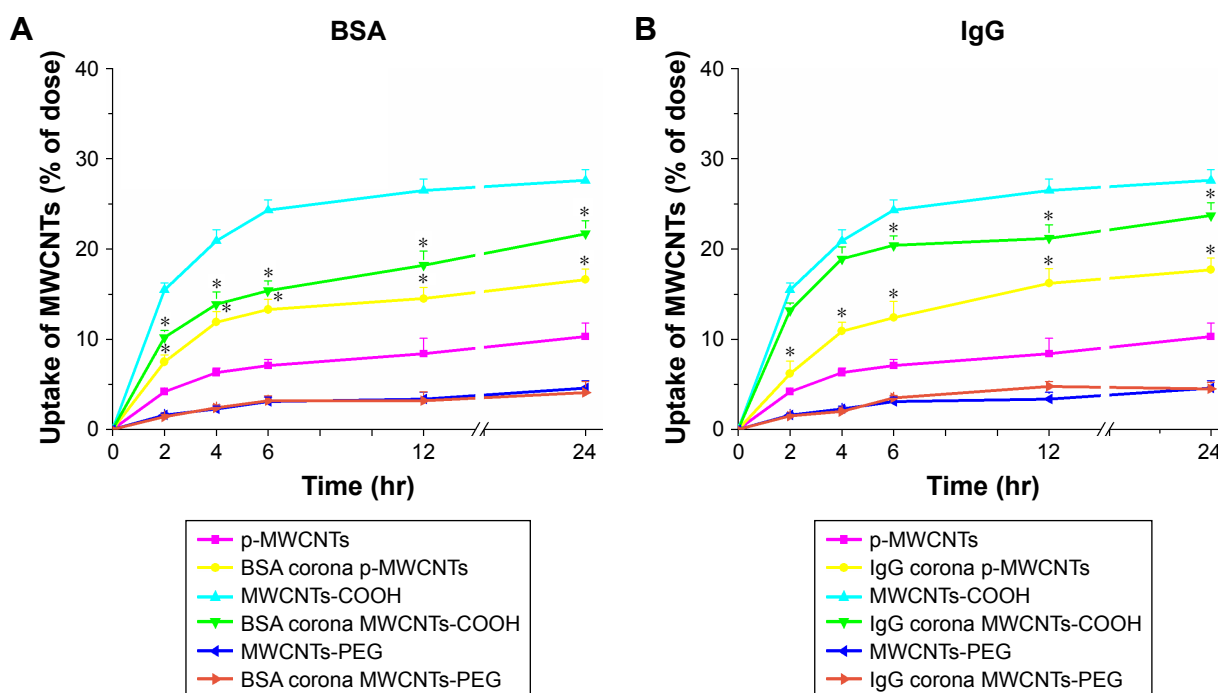


**Figure 3** Cellular uptake of three types of MWCNTs with or without BSA (A) and IgG (B) coronas by RAW264.7 cells.

**Notes:** Quantitative analysis of cellular uptake of MWCNTs by RAW264.7 cells as shown by the standard turbidimetric method. Cells were cultured in 6-well culture dishes to confluence and exposed to MWCNTs (25  $\mu\text{g}/\text{mL}$ ) up to 24 hours. Dimethyl sulfoxide (0.2 mL) was added to each well and the lysate was pipetted thoroughly. A 250  $\mu\text{L}$  sample was transferred to 96-well plates, and the OD (640 nm) was measured to quantify the amount of cell-associated MWCNTs. Data are representative of three independent experiments. \* $P < 0.05$  compared to the same types of MWCNTs without protein corona BSA: human plasma protein; IgG: human serum albumin.

**Abbreviations:** IgG, immunoglobulin G; MWCNTs, multiwalled carbon nanotubes; MWCNTs-COOH, carboxylated MWCNTs; MWCNTs-PEG, polyethylene glycol MWCNTs.

IgG-coated pristine MWCNTs. To assess cell status, we examined morphology after either incubation with MWCNTs in FBS or FBS alone to determine the effect of protein corona. Well-shaped cells that were round, lucent, and well attached were observed for RAW264.7 cells without MWCNT treatment (Figure 4C). No apparent morphological transformation was observed after incubation with MWCNTs-PEG either in FBS or FBS-free medium for 6 hours. However, following incubation with MWCNTs-COOH or pristine MWCNTs, the numbers of adherent and viable cells gradually decreased, and the cells and MWCNTs were gathered in clusters. There

was a tendency of agglomerates to adhere to cell walls, and we observed cell membrane shrinkage and cytosolic vacuole formation following exposure to MWCNTs-COOH and pristine MWCNTs.

### Inflammatory response to MWCNTs-protein corona in RAW264.7 cells

To assess the influence of protein adsorption on inflammatory cytokine production, IL-1 $\beta$  and TNF- $\alpha$  were measured (Figure 5). Our results showed that pristine MWCNTs and MWCNTs-COOH significantly affected biological responses

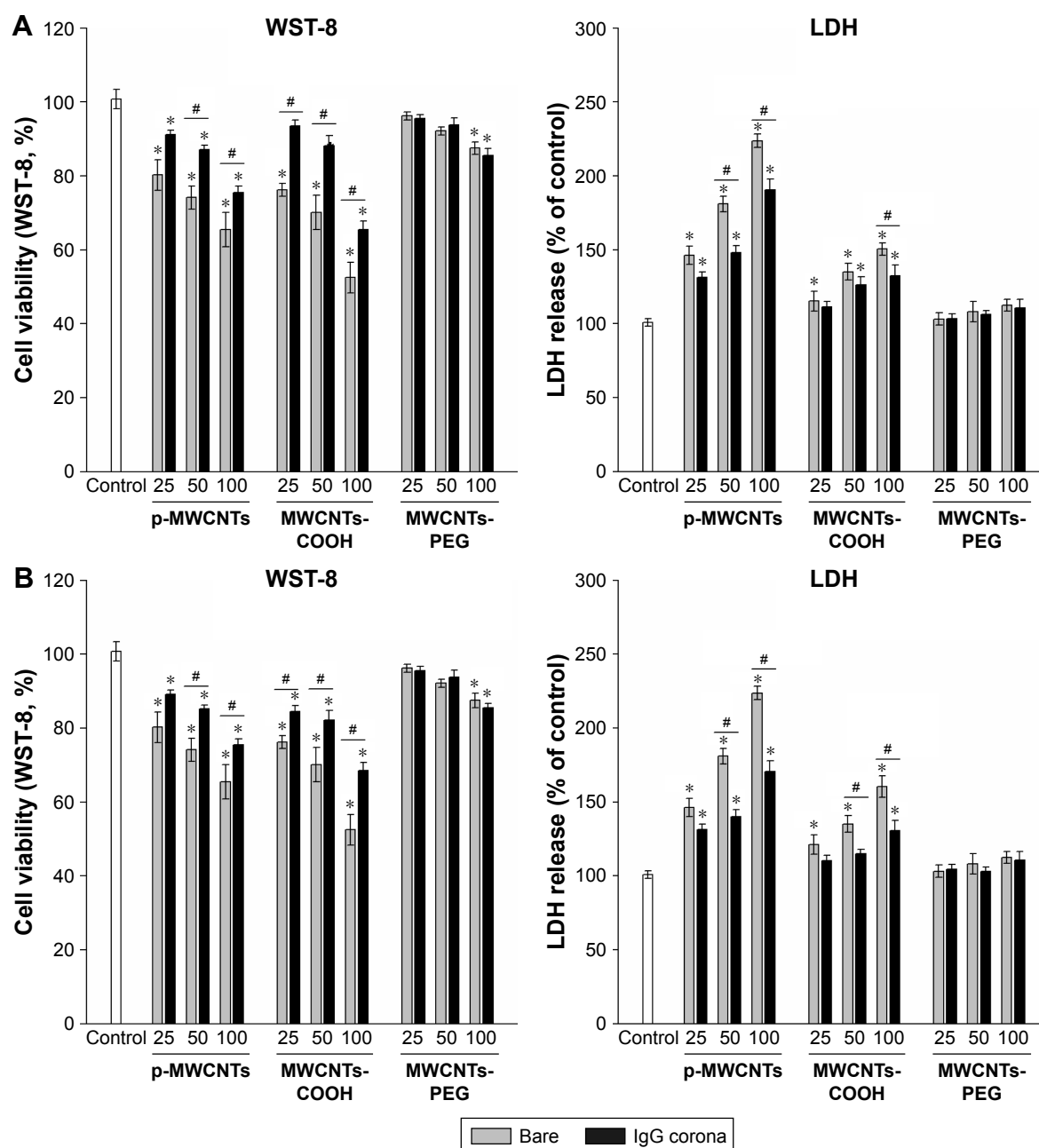
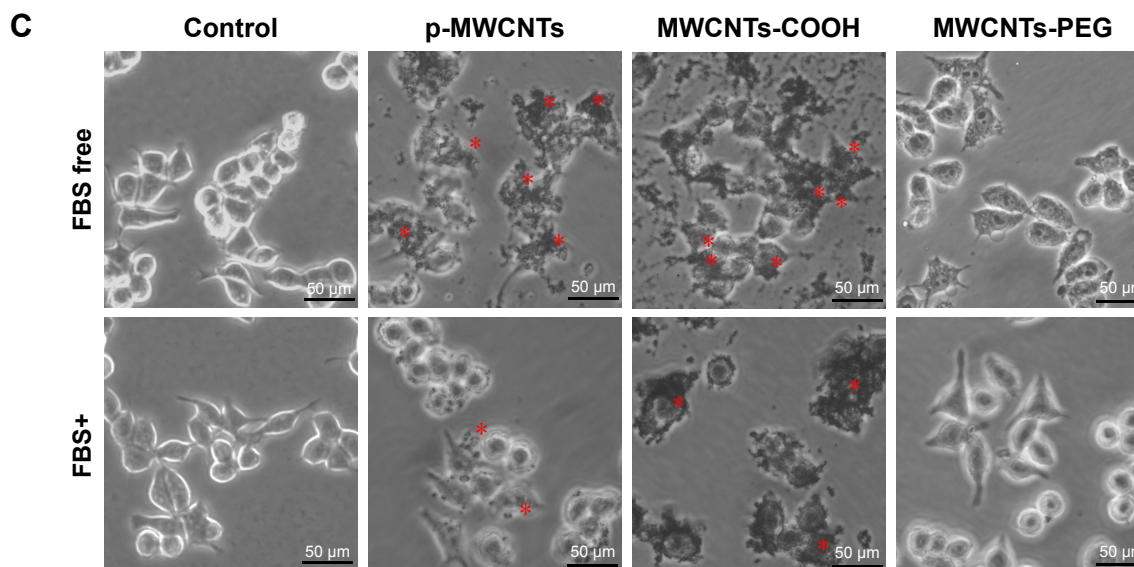


Figure 4 (Continued)





**Figure 4** Cytotoxicity in RAW264.7 cells exposed to three types of MWCNTs with or without BSA (A) and IgG (B) coronas.

**Notes:** Assessment of cytotoxicity of MWCNTs with WST-8 and LDH assays. After exposure to 25, 50, and 100 µg/mL of each of the MWCNT suspensions for 24 hours, RAW264.7 cells were incubated with the WST-8 reagent for 1 hour, and the absorbance was measured at 490 nm. All the WST-8 values were normalized according to the control (no MWCNT exposure), which was regarded as the 100% cell viability reference point. Similar to the treatment, cell supernatants from control and exposure experiments were collected and assayed for LDH activity as described in the Materials and methods section. Data are representative of three separate experiments with at least three wells per treatment. All the WST-8 and LDH values were normalized according to the nontreated control, which was regarded as representing 100% cell viability. \* $P < 0.05$  compared to control cells, # $P < 0.05$  compared to the same types of MWCNTs without protein corona. (C) Morphology of RAW264.7 cells treated with three types of MWCNTs (25 µg/mL) in FBS free and complete medium for 6 hours. The asterisks indicate MWCNTs agglomerates to adhere to cell walls and shrinkage of the cell membrane. The scale bar is 50 µm.

**Abbreviations:** IgG, immunoglobulin G; LDH, lactate dehydrogenase; MWCNTs, multiwalled carbon nanotubes; MWCNTs-COOH, carboxylated MWCNTs; MWCNTs-PEG, polyethylene glycol MWCNTs.

in terms of IL-1 $\beta$  and TNF- $\alpha$  production by RAW264.7 cells at the “low toxic” level (25 µg/mL) but did not induce significant cell death. Interestingly, we found that BSA binding significantly increased IL-1 $\beta$  and TNF- $\alpha$  release induced by pristine MWCNTs, but BSA binding reduced the production of IL-1 $\beta$  and TNF- $\alpha$  induced by MWCNTs-COOH, suggesting that BSA binding can modulate CNT bioactivity.

### Role of frustrated phagocytosis in protein corona-dependent cytotoxicity and inflammatory factor release

To investigate the impact of MWCNT protein corona on phagocytosis and macrophage activation, cells were pretreated with CytoD, an actin barbed-end capping molecule, to disrupt phagocytosis. The results showed that uptake of bare and coronated pristine MWCNTs and MWCNTs-COOH significantly decreased after pretreatment with CytoD, and MWCNTs-COOH and BSA coronated pristine MWCNTs showed 69% and 43% inhibition relative to control, respectively. However, CytoD did not influence RAW264.7 phagocytic uptake of MWCNTs-PEG cells (Figure 6A). Additionally, we measured cell viability, LDH release, and IL-1 $\beta$  to verify the hypothesis that corona-dependent cytotoxicity and pro-inflammatory effects were due to nanotube

phagocytosis. CytoD treatment increased cell viability and reduced IL-1 $\beta$  production caused by exposure to pristine MWCNTs and MWCNTs-COOH (Figure 6B and D), but it had no significant decrease in LDH release (Figure 6C).

### Discussion

Proteins adsorb onto NPs in the form of protein corona in biological environments. This event affects NP properties, changes protein structure, and impacts NP behavior in the biological milieu. In the current study, we investigated the role of MWCNT surface chemistry on BSA and IgG adsorption behavior and spatial configuration. We further explored MWCNT effects on cellular uptake, cytotoxicity, and cellular responses in RAW264.7 macrophages. Pristine MWCNTs are not water soluble because of the hydrophobic graphite sheet, and we did find that BSA and IgG binding decreased their hydrodynamic size. Adsorption of protein molecules on nanotube surfaces can increase water solubility and dispersibility of pristine MWCNTs by changing the surface tension of a pristine water–nanotube interface,<sup>16</sup> and the similar phenomenon of protein binding increased water solubility and dispersibility, which has been commonly observed in other carbon nanomaterials such as single-walled CNTs and graphene oxide.<sup>17,18</sup> In contrast to decreased size for pristine

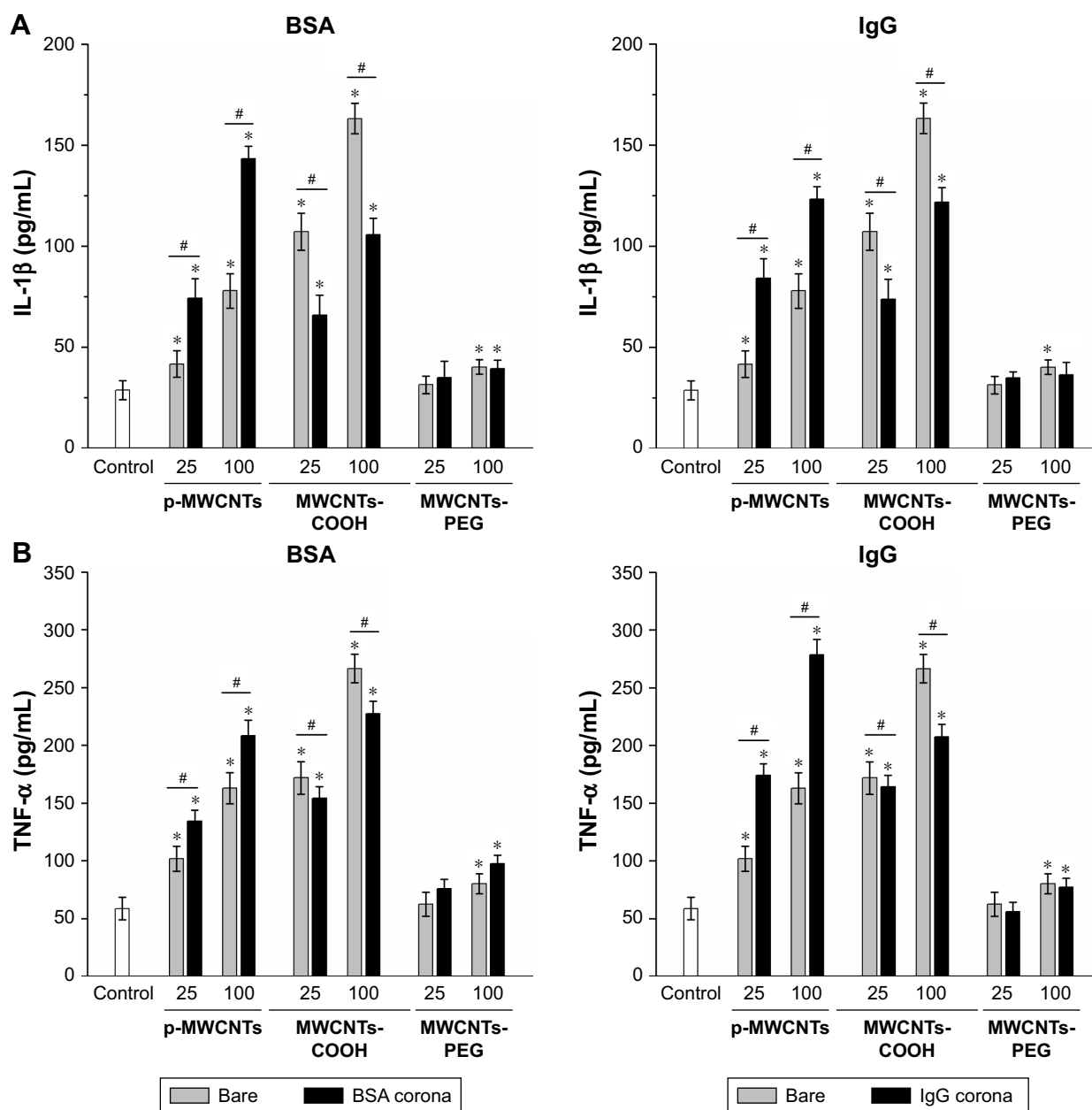


**Figure 5** Pro-inflammatory cytokine production in RAW264.7 cells in response to three types of MWCNTs with or without BSA and IgG coronas.

**Notes:** IL-1 $\beta$  (A) and TNF- $\alpha$  (B) production in RAW264.7 cells. RAW264.7 cells were exposed to 0, 25, and 100  $\mu$ g/mL MWCNTs with or without BSA and IgG coronas for 24 hours to determine IL-1 $\beta$  and TNF- $\alpha$  release into the supernatants was assessed by ELISA. Control cells were not subjected to MWCNTs exposure. \* $P$ <0.05 compared to control cells, # $P$ <0.05 compared to the same types of MWCNTs without protein corona.

**Abbreviations:** IgG, immunoglobulin G; MWCNTs, multiwalled carbon nanotubes; MWCNTs-COOH, carboxylated MWCNTs; MWCNTs-PEG, polyethylene glycol MWCNTs; TNF- $\alpha$ , tumor necrosis factor  $\alpha$ .

MWCNTs in BSA and IgG media by ~34% to 45%, the sizes of the MWCNTs-COOH in BSA and IgG media were slightly increased, probably due to protein adsorption. Protein corona formed on NPs are dependent on the NP-protein interaction, and NP-protein complexes lead to an increase of NP core size.<sup>19</sup> The existing literature indicates that protein adsorption to the NP surface could change its native charge; the zeta potential of all MWCNTs was less negative compared

to that of samples dispersed in water but remained negative in protein medium. Proteins contain positively charged patches of arginine and lysine; the electrostatic force between the negative charge on the MWCNT-COOH surface and the positively charged patches contributes to the increase in zeta potential.<sup>20</sup>

The adsorption of proteins on NPs has important implications in nanomedicine. The present study revealed the

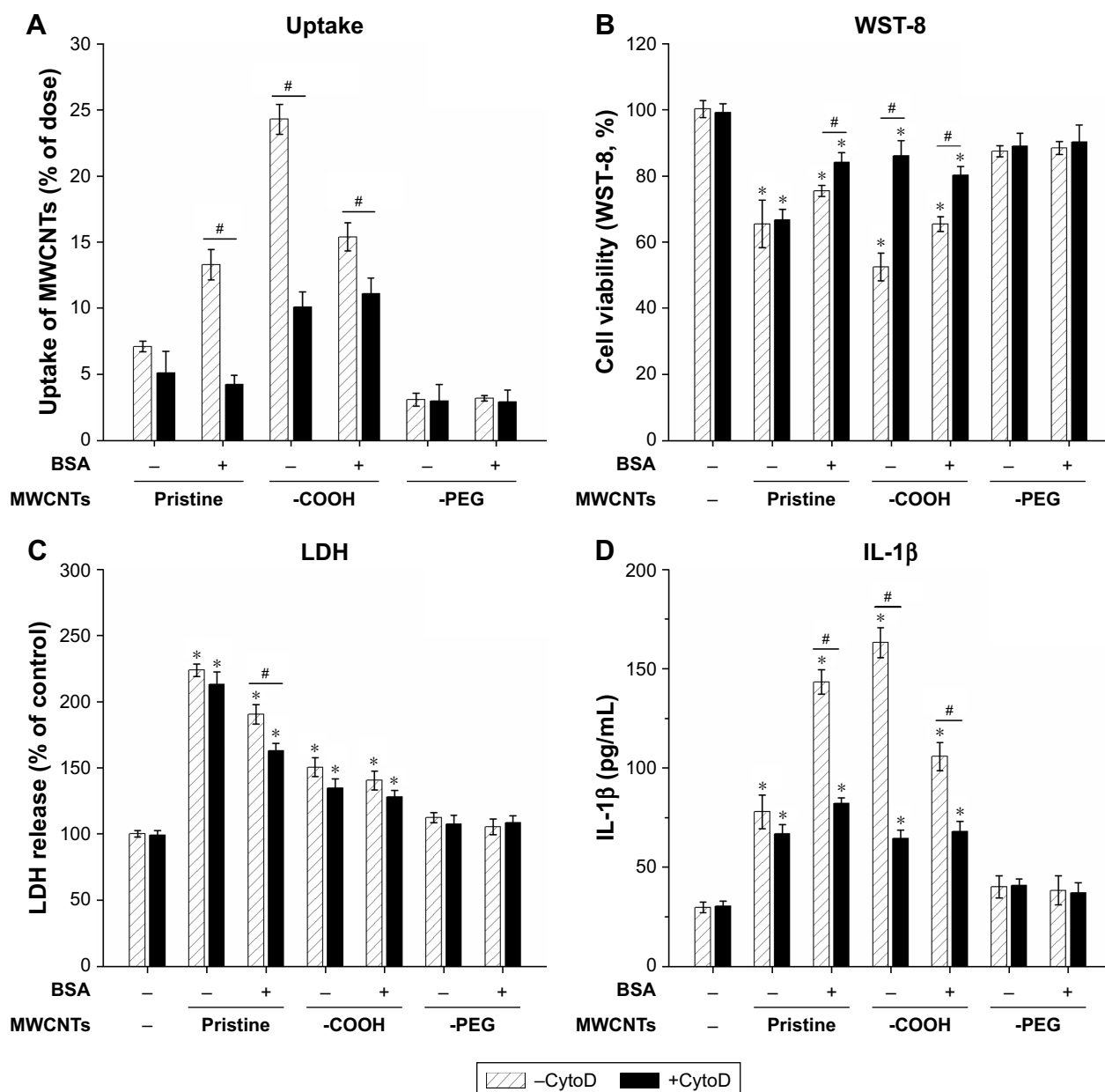


**Figure 6** Inhibition of endocytosis by cytochalasin D that attenuates the toxicity of MWCNTs.

**Notes:** Raw264.7 cells preincubated with endocytosis inhibitor, Cytochalasin D (CytoD) for 2 hours, and investigated the cellular uptake, cytotoxicity and pro-inflammatory cytokine secretion after 4  $\mu$ M CytoD inhibitor pretreatment with bare or BSA coronas MWCNTs. (A) Cellular uptake of Raw264.7 cells was analyzed after the treatment of MWCNTs for 6 hours. Cytotoxicity was measured by WST-8 (B) and LDH assays (C). Levels of IL-1 $\beta$  (D) of RAW264.7 cells at 24 hours following the treatment. All assays were performed as described in Materials and methods section. Control cells were not subjected to MWCNTs exposure. \* $P$ <0.05 compared to control cells, <sup>#</sup> $P$ <0.05 compared to the same types of MWCNTs with CytoD inhibitor pretreatment.

**Abbreviations:** IgG, immunoglobulin G; LDH, lactate dehydrogenase; MWCNTs, multiwalled carbon nanotubes; MWCNTs-COOH, carboxylated MWCNTs; MWCNTs-PEG, polyethylene glycol MWCNTs.

adsorption capacity of pristine MWCNTs to be three times greater than MWCNTs-COOH and eight-fold higher than MWCNTs-PEG coronas, implying that the physical and chemical features of different functional MWCNTs might also affect protein adsorption. It is commonly reported that both electrostatic and hydrophobic interactions are major driving forces for proteins adsorbed on MWCNTs. Strong

$\pi$ - $\pi$  stacking interactions between pristine MWCNTs and aromatic protein residues play a vital role in the binding capacity of adsorption on CNTs. In addition, hydrophobic or charged surfaces tend to adsorb more proteins and denature them to a greater extent than neutral and hydrophilic surfaces.<sup>21</sup> This might explain why there were higher amounts of BSA and IgG corona formed on pristine MWCNTs.

However, NPs with a negative surface charge had a lower tendency to bind to proteins with an isoelectric point ( $pI$ )  $\leq 7.4$ , thus explaining the possibly lower amounts of BSA ( $pI \sim 4.9$ ) and IgG ( $pI$  6.1–8.5) corona formed on MWCNTs-COOH. It should be noted that PEGylation reduces but does not totally prevent protein adsorption on the NP surface,<sup>22</sup> thus explaining the lowest amount of BSA adsorption on MWCNTs-PEG. This corresponds with the results of an adsorption behavior study, wherein coated PEG chains effectively resisted the adsorption of proteins and decreased cell attachment to modified surfaces.<sup>23</sup> On the other hand, comparing the adsorption capacity of two proteins for the same MWCNTs, the amount of bound IgG was significantly higher than that of BSA at the same time point. This may be due to different properties of the two proteins, such as repulsion between counter charges. The  $pI$ s of BSA and IgG are mainly in the acidic and neutral range under physiological conditions. Being positively charged ( $pI$  6.1–8.5), IgG showed higher binding for the negative charge of MWCNTs-COOH due to electrostatic attraction and hydrophobic interactions.<sup>24</sup> This correlates well with adsorption behavior studies, where more hydrophobic or negatively charged surfaces facilitate protein interaction.

To a certain extent, interactions between MWCNTs and proteins change the properties and structures of adsorbed proteins. Intrinsic fluorescence from proteins is due to photoexcitation of tryptophan, tyrosine, and phenylalanine.<sup>25</sup> The binding of ligands to proteins frequently causes changes structural changes that alter the intrinsic or extrinsic fluorophore in the protein, resulting in measurable changes in the fluorescence spectrum.<sup>26</sup> The fluorescence intensity of tryptophan was quenched by different types of MWCNTs, and a blue shift was measured in the presence of -COOH and pristine MWCNTs. This indicates that the fluorescence chromophores of BSA and IgG were placed in a more hydrophobic environment in the presence of MWCNTs. The fluorescence intensity decreased after the addition of all three types of MWCNTs, suggesting that interaction of MWCNTs with BSAs and IgG resulted in fluorescence quenching of surface-exposed tryptophan residues in BSA and IgG, which led to the formation of nonfluorescent complexes. Based on the difference in the absorption of left and right circularly polarized light, CD spectra were used to measure adsorbed protein secondary structures in aqueous solutions. BSA and IgG are most compact in their native forms. Upon adsorption to the MWCNT surface, the molecules undergo expansion, which may result in loss of biological activity or immune response activation. This is consistent with the quantitative results of CNT and protein adsorption in our study.

It is important to note that intracellular uptake and serum factors are crucial determinants for toxicity, recognition, and phagocytosis. We found that the cellular uptake of MWCNTs-COOH was higher than that for pristine MWCNTs, and BSA and IgG coronas significantly increased the uptake of pristine MWCNTs by RAW264.7 cells. Similarly, Wang et al<sup>27</sup> found that BSA could act as an effective dispersant for purified MWCNTs and as-prepared MWCNTs in various tissue culture media. They proposed that better nanotube dispersal could increase the local dosimetry, resulting in increased contact of nanotubes with cellular membranes.<sup>27</sup> Improved dispersion can enhance cellular uptake due to improved cellular dosimetry. However, we found that cellular uptake of MWCNTs-COOH corona was lower for bare MWCNTs-COOH, and protein coating reduced the cellular uptake of MWCNTs-COOH. As a foreign material, NPs are quickly recognized by the immune system after entering the body. Macrophages play a dominant role in NP recognition, phagocytosis, and clearing. Serum factors also affect recognition and phagocytosis. BSA is often referred to as a dysopsonin, a protein corona enriched with dysopsonins that prolongs circulation times and diminishes uptake by host macrophages.<sup>28</sup> As opsonins, immunoglobulins bind to receptors on macrophages and elicit phagocytosis. However, we found that the opsonin-rich protein corona did not increase MWCNT uptake by RAW264.7 cells. These results support those of another group, indicating that protein absorption onto silica and gold NPs decreased cellular uptake.<sup>29</sup> In addition, we found low cellular uptake of MWCNTs-PEG, and that protein coating did not have a significant effect. This suggests that nonspecific binding of NPs to protein results in slower, reduced NP uptake.

Dose-dependent decreases in cell viability were observed after treatment with the three types of MWCNTs, and the effects of the different functional groups and protein corona of MWCNTs on cell viability were significant. We previously showed that MWCNT-induced toxicity induced is highly dependent on their functionalization.<sup>12</sup> In this study, we focused on the influence of the protein corona on cell viability and found that pristine MWCNTs and MWCNTs-COOH alone or BSA-coronated MWCNTs induced significant and dose-dependent cell death in macrophages. At the same dose, the viability of cells exposed to bare pristine MWCNTs and MWCNTs-COOH was significantly decreased compared to that of cells treated with BSA coronated MWCNTs, but protein corona did not significantly affect the viability of cells exposed to MWCNTs-PEG. The effect of IgG on MWCNT cytotoxicity had a similar order as observed for

MWCNT binding capacity. There was a significant increase in the viability of cells for pristine MWCNTs and MWCNTs-COOH by adsorption of IgG, indicating that more protein adsorbed led to a smaller decrease in cell viability. It could be concluded that BSA and IgG caused less cytotoxicity by forming MWCNT-protein corona. These findings are consistent with results obtained from previous studies that NPs-protein conjugates decreased the biological toxicity of these particles.<sup>30–33</sup> Protein corona on CNTs results in fewer surfaces exposed to media and limits interaction with cells; thus, fewer reactive oxygen species or inflammatory factors may be produced. For this reason, protein binding is a key factor for reducing toxicity. Distinct from MWCNTs-PEG, proteins rapidly coat the surface of pristine MWCNTs and MWCNT-COOH with more compact forms that are more effective at protecting cells from the CNT surface. To further investigate the influence of protein adsorption on the cytotoxicity of different types of MWCNTs, we measured LDH release. MWCNTs dose-dependently increased the release of LDH after 24 hours. At the same dose, MWCNTs-COOH with or without protein corona led to a higher LDH release; this was reduced in protein-coronated MWCNTs-COOH, but only treatment with 100 µg/mL was significant compared to that of bare MWCNTs-COOH. Pristine MWCNTs caused significant cell membrane damage compared to that of BSA- and IgG-coated pristine MWCNTs, which was inconsistent with cell viability measured in the presence of bare and protein-coronated pristine MWCNTs. The discrepant results between the two cytotoxicity assays are mainly due to the nature of each assay. The LDH assay is based on measurement of LDH levels to quantify cell membrane damage after necrosis and cell death (final stages of the cell death process), whereas the WST-8 assay measures mitochondrial activity that detects earlier and more subtle changes in mitochondria.<sup>34</sup> Previous studies suggested that MWCNTs-COOH attenuate the cytotoxicity by forming holes in the cell membrane.<sup>35,36</sup> In addition, our previous TEM investigation revealed that highly dispersed MWCNTs-COOH can cross membranes to enter cells, while pristine MWCNTs damage the cell membrane and decrease its integrity.<sup>13</sup> These findings indicate different mechanisms of penetration and intracellular accumulation that are linked to both surface functionalization and protein corona, which could alter interactions between CNTs and cell membranes. Functional modification and protein adsorption of pristine MWCNTs could increase their solubility and allow them to cross the membrane without damaging cells. The morphology of cells incubated with MWCNTs in either FBS or FBS-free medium

revealed shrinkage of the cell membrane and vacuole formation following exposure to MWCNTs-COOH and pristine MWCNTs, suggesting that they increase cytotoxicity. In addition, cells treated with MWCNTs-COOH had better adherence and higher refractivity compared to those treated with protein-coronated MWCNTs-COOH.

NP uptake can occur through phagocytosis, and this event is followed by macrophage activation and cytokine release. Our results showed that pristine MWCNTs and MWCNTs-COOH significantly affected biological responses in terms of IL-1 $\beta$  and TNF- $\alpha$  production in RAW264.7 cells at the “low toxic” level without inducing significant cell death. However, these treatments may impact cell homeostasis and activate cell biological responses. Interestingly, we found that BSA binding remarkably enhanced IL-1 $\beta$  and TNF- $\alpha$  release by pristine MWCNTs, but BSA binding reduced IL-1 $\beta$  and TNF- $\alpha$  production by MWCNTs-COOH, suggesting that BSA binding can modulate CNT bioactivity. After proteins adsorbed to the NP surface, protein conformational changes result in unnatural protein configurations that trigger phagocytosis and potential inflammatory reactions.<sup>24,37,38</sup> We observed comparatively higher IL-1 $\beta$  and TNF- $\alpha$  production for BSA-coronated pristine MWCNTs and bare MWCNTs-COOH. This result supports the cellular uptake study, where uptake was higher than that of the bare pristine MWCNTs and protein-coronated MWCNTs-COOH. This might be due to increased cell uptake of MWCNTs-COOH in RAW264.7 cells, leading to disturbed intracellular balance and cell stress, thus inducing pro-inflammatory cytokine production. At the same time, our study revealed that highly dispersed bare MWCNTs-COOH were able to cross the cell membrane and damage its structural integrity. This results in the release of pro-inflammatory mediators. The presence of BSA and IgG corona significantly reduced the uptake of MWCNTs-COOH, thereby causing IL-1 $\beta$  and TNF- $\alpha$  secretion to be dramatically reduced compared to that of bare MWCNTs-COOH. All of these results suggest that the presence of a protein corona with MWCNTs could significantly suppress the inflammatory effects, making it more biocompatible for biomedical applications. As protein coronas decrease MWCNT uptake, this could reduce intracellular oxidative stress, but it might also decrease surface reactivity by providing a more biocompatible surface. Collectively, these results indicate that protein corona with MWCNTs reduces cellular uptake, decreases cytotoxicity, and also significantly reduces the inflammatory effect within cells.

A previous study reported that cellular uptake of CNTs takes place in phagocytosis, endocytosis, or diffusion.<sup>39</sup>

In an attempt to investigate the impact of MWCNT protein corona on phagocytosis/endocytosis and macrophage activation, cells were pretreated with an actin barbed-end capping molecule, CytoD, to disrupt phagocytosis and endocytosis. Uptake of bare and coronated pristine MWCNTs and MWCNTs-COOH was significantly reduced after CytoD pretreatment but did not influence the phagocytic uptake of MWCNTs-PEG by RAW264.7 cells. Additionally, we demonstrated that CytoD inhibited macrophage phagocytosis of MWCNTs, leading to increased cell viability and decreased pro-inflammatory cytokine release from RAW264.7 cells, which confirmed that frustrated phagocytosis plays key roles in reducing cell survival and leading to inflammation in the case of CNTs. Because the properties of PEG prevent cellular uptake and protein adsorption, there was less uptake of MWCNTs-PEG by macrophages, and this led to nonobvious cytotoxicity and a pro-inflammatory reaction after exposure. Our results also indirectly demonstrated the importance of particle uptake and the role of frustrated phagocytosis in pro-inflammatory cytokine release from MWCNT-exposed macrophages as initiating cytotoxic events. Notably, we did not observe a significant decrease in LDH release. The pristine MWCNTs and MWCNTs-COOH samples induced an obvious increase in LDH during the initial treatments with CytoD, due to reduced cell membrane adhesion. We speculated that MWCNTs physically induce dysfunction directly through their interaction with the plasma membrane. This was demonstrated by a group that suggested that MWCNTs induced direct physical damage to cell membranes and this led to macrophage cytotoxicity.<sup>40</sup> Here we showed that phagocytosis is the major mechanism responsible for the internalization of MWCNTs with or without protein coating. The combination of MWCNT physical and chemical properties and the effects of protein corona on the biological behavior of MWCNTs are important for assessing biological interactions and may provide insight into the design of safe surfaces for functional CNTs to be used in biological applications and to fully assess their toxic effects.

## Conclusion

Taken together, our findings indicate that BSA and IgG adsorbed on three types of MWCNTs. This not only changed the diameters and zeta potentials of MWCNTs, but also resulted in loss of the original protein structure, which may influence its behavior and lead to potential hazardous effects in macrophages. The adsorption capacity and further changes in proteins, cytotoxicity, and pro-inflammatory response were dependent on the physicochemical properties

of MWCNTs. Cellular uptake and frustrated phagocytosis are key initiating events in the pro-inflammatory response of MWCNT-exposed macrophages. Overall, our study improves our understanding of the mechanisms responsible for interactions between MWCNTs and proteins, which could inform the design of safe surfaces of functional CNTs with minimal toxicity.

## Acknowledgment

This work was supported by the Natural Science Foundation of China (grant numbers 81673218, 81302461, and the and 31671034), Research Fund for the Doctoral Program of Higher Education (grant number 20130092120062).

## Disclosure

The authors report no conflicts of interest in this work.

## References

1. Alshehri R, Ilyas AM, Hasan A, Arnaout A, Ahmed F, Memic A. Carbon nanotubes in biomedical applications: factors, mechanisms, and remedies of toxicity. *J Med Chem*. 2016;59(18):8149–8167.
2. Liu Y, Zhao Y, Sun B, Chen C. Understanding the toxicity of carbon nanotubes. *Acc Chem Res*. 2013;46(3):702–713.
3. Francis AP, Devasena T. Toxicity of carbon nanotubes: a review. *Toxicol Ind Health*. 2018;34(3):200–210.
4. Madani SY, Mandel A, Seifalian AM. A concise review of carbon nanotube's toxicology. *Nano Rev*. 2013;4(1):21521.
5. Lin D, Xing B. Adsorption of phenolic compounds by carbon nanotubes: role of aromaticity and substitution of hydroxyl groups. *Environ Sci Technol*. 2008;42(19):7254–7259.
6. Wang X, Qu R, Liu J, et al. Effect of different carbon nanotubes on cadmium toxicity to *Daphnia magna*: the role of catalyst impurities and adsorption capacity. *Environ Pollut*. 2016;208(Pt B):732–738.
7. Wang X, Qu R, Huang Q, Wei Z, Wang Z. Hepatic oxidative stress and catalyst metals accumulation in goldfish exposed to carbon nanotubes under different pH levels. *Aquat Toxicol*. 2015;160:142–150.
8. Rahman L, Jacobsen NR, Aziz SA, et al. Multi-walled carbon nanotube-induced genotoxic, inflammatory and pro-fibrotic responses in mice: investigating the mechanisms of pulmonary carcinogenesis. *Mutat Res*. 2017;823:28–44.
9. Bhattacharya K, Mukherjee SP, Gallud A, et al. Biological interactions of carbon-based nanomaterials: from coronation to degradation. *Nanomedicine*. 2016;12(2):333–351.
10. Corbo C, Molinaro R, Parodi A, Toledano Furman NE, Salvatore F, Tasciotti E. The impact of nanoparticle protein corona on cytotoxicity, immunotoxicity and target drug delivery. *Nanomedicine*. 2016;11(1):81–100.
11. Long J, Li X, Kang Y, Ding Y, Gu Z, Cao Y. Internalization, cytotoxicity, oxidative stress and inflammation of multi-walled carbon nanotubes in human endothelial cells: influence of pre-incubation with bovine serum albumin. *RSC Advances*. 2018;8(17):9253–9260.
12. Zhang T, Tang M, Kong L, et al. Comparison of cytotoxic and inflammatory responses of pristine and functionalized multi-walled carbon nanotubes in RAW 264.7 mouse macrophages. *J Hazard Mater*. 2012;219–220:203–212.
13. Zhang T, Tang M, Kong L, et al. Surface modification of multiwall carbon nanotubes determines the pro-inflammatory outcome in macrophage. *J Hazard Mater*. 2015;284:73–82.
14. Zhang T, Tang M, Zhang S, et al. Systemic and immunotoxicity of pristine and PEGylated multi-walled carbon nanotubes in an intravenous 28 days repeated dose toxicity study. *Int J Nanomedicine*. 2017;12:1539–1554.

15. Zhang T, Qian L, Tang M, et al. Evaluation on cytotoxicity and genotoxicity of the L-glutamic acid coated iron oxide nanoparticles. *J Nanosci Nanotechnol*. 2012;12(3):2866–2873.
16. Zeinabad HA, Zarrabian A, Saboury AA, Alizadeh AM, Falahati M. Interaction of single and multi wall carbon nanotubes with the biological systems: Tau protein and PC12 cells as targets. *Sci Rep*. 2016; 6(1):26508.
17. Bai W, Wu Z, Mitra S, Brown JM. Effects of multiwalled carbon nanotube surface modification and purification on bovine serum albumin binding and biological responses. *J Nanomater*. 2016;2016(2):1–10.
18. Hu W, Peng C, Lv M, et al. Protein corona-mediated mitigation of cytotoxicity of graphene oxide. *ACS Nano*. 2011;5(5):3693–3700.
19. Cheng X, Tian X, Wu A, et al. Protein corona influences cellular uptake of gold nanoparticles by phagocytic and nonphagocytic cells in a size-dependent manner. *ACS Appl Mater Interfaces*. 2015;7(37): 20568–20575.
20. Treuel L, Docter D, Maskos M, Stauber RH. Protein corona – from molecular adsorption to physiological complexity. *Beilstein J Nanotechnol*. 2015;6:857–873.
21. Lindman S, Lynch I, Thulin E, Nilsson H, Dawson KA, Linse S. Systematic investigation of the thermodynamics of HSA adsorption to *N*-iso-propylacrylamide/*N*-tert-butylacrylamide copolymer nanoparticles. Effects of particle size and hydrophobicity. *Nano Lett*. 2007;7(4): 914–920.
22. Pozzi D, Colapicchioni V, Caracciolo G, et al. Effect of polyethylene glycol (PEG) chain length on the bio-nano-interactions between PEGylated lipid nanoparticles and biological fluids: from nanostructure to uptake in cancer cells. *Nanoscale*. 2014;6(5):2782–2792.
23. Zhang M, Desai T, Ferrari M. Proteins and cells on PEG immobilized silicon surfaces. *Biomaterials*. 1998;19(10):953–960.
24. Aggarwal P, Hall JB, McLeland CB, Dobrovolskaia MA, McNeil SE. Nanoparticle interaction with plasma proteins as it relates to particle biodistribution, biocompatibility and therapeutic efficacy. *Adv Drug Deliv Rev*. 2009;61(6):428–437.
25. Papadopoulou A, Green RJ, Frazier RA. Interaction of flavonoids with bovine serum albumin: a fluorescence quenching study. *J Agric Food Chem*. 2005;53(1):158–163.
26. Chi Z, Liu R, Teng Y, Fang X, Gao C. Binding of oxytetracycline to bovine serum albumin: spectroscopic and molecular modeling investigations. *J Agric Food Chem*. 2010;58(18):10262–10269.
27. Wang X, Xia T, Ntim SA, et al. Quantitative techniques for assessing and controlling the dispersion and biological effects of multiwalled carbon nanotubes in mammalian tissue culture cells. *ACS Nano*. 2010;4(12): 7241–7252.
28. Nguyen VH, Meghani NM, Amin HH, et al. Modulation of serum albumin protein corona for exploring cellular behaviors of fattigation-platform nanoparticles. *Colloids and Surfaces B: Biointerfaces*. 2018; 170:179–186.
29. Mirshafiee V, Kim R, Park S, Mahmoudi M, Kraft ML. Impact of protein pre-coating on the protein corona composition and nanoparticle cellular uptake. *Biomaterials*. 2016;75:295–304.
30. Lu N, Sui Y, Ding Y, Tian R, Li L, Liu F. Adsorption of human serum albumin on functionalized single-walled carbon nanotubes reduced cytotoxicity. *Chem Biol Interact*. 2018;295:64–72.
31. Saikia J, Yazdimamaghani M, Hadipour Moghaddam SP, Ghandehari H. Differential protein adsorption and cellular uptake of silica nanoparticles based on size and porosity. *ACS Appl Mater Interfaces*. 2016;8(50): 34820–34832.
32. Bai J, Wang T, Wang Y, Jiang X. Effects of nanoparticle surface ligands on protein adsorption and subsequent cytotoxicity. *Biomater Sci*. 2014;2(4):493–501.
33. Zhao X, Lu D, Hao F, Liu R. Exploring the diameter and surface dependent conformational changes in carbon nanotube-protein corona and the related cytotoxicity. *J Hazard Mater*. 2015;292:98–107.
34. Fotakis G, Timbrell JA. In vitro cytotoxicity assays: comparison of ldh, neutral red, MTT and protein assay in hepatoma cell lines following exposure to cadmium chloride. *Toxicol Lett*. 2006;160(2):171–177.
35. Fanizza C, Casciardi S, Inconato F, et al. Human epithelial cells exposed to functionalized multiwalled carbon nanotubes: interactions and cell surface modifications. *J Microsc*. 2015;259(3):173–184.
36. Cavallo D, Fanizza C, Ursini CL, et al. Multi-walled carbon nanotubes induce cytotoxicity and genotoxicity in human lung epithelial cells. *J Appl Toxicol*. 2012;32(6):454–464.
37. Dobrovolskaia MA, McNeil SE. Immunological properties of engineered nanomaterials. *Nat Nanotechnol*. 2007;2(8):469–478.
38. Dobrovolskaia MA, Aggarwal P, Hall JB, Mcneil SE. Preclinical studies to understand nanoparticle interaction with the immune system and its potential effects on nanoparticle biodistribution. *Mol Pharm*. 2008;5(4):487–495.
39. Raffa V, Ciofani G, Vittorio O, Riggio C, Cuschieri A. Physicochemical properties affecting cellular uptake of carbon nanotubes. *Nanomedicine*. 2010;5(1):89–97.
40. Shimizu K, Uchiyama A, Yamashita M, Hirose A, Nishimura T, Oku N. Biomembrane damage caused by exposure to multi-walled carbon nanotubes. *J Toxicol Sci*. 2013;38(1):7–12.

## Supplementary materials

### Synthesis and characterization of MWCNTs

#### Method

The pristine MWCNTs (p-MWCNTs) obtained as powder from Shenzhen Nano Harbor Co. had an average diameter ranging from 10 to 20 nm, a length range of 5–15  $\mu\text{m}$  and a purity of >95%. The MWCNTs with carboxylation (COOH)- or polyethylene glycol (PEG)- were synthesized by two steps. In the first step, we used p-MWCNTs to prepare carboxyl (COOH)-functionalized MWCNTs through oxidization. Then the PEG modification was introduced by esterification of the acylated COOH-MWCNTs with polyethylene glycol. The characterization of three types of MWCNTs (pristine MWCNTs, MWCNTs-COOH, and MWCNTs-PEG) was carried out using procedures previously described.<sup>11</sup> The samples (pristine MWCNTs, MWCNTs-COOH, MWCNTs-PEG) were characterized by Fourier transform infrared spectroscopy (FTIR; PerkinElmer Inc., Waltham, MA, USA), and validated with thermogravimetric analysis (PE Pyris 1 TGE; PerkinElmer Inc.).

## Results

### FTIR spectroscopy

Figure S1 shows the FTIR spectra of pristine and functionalized MWCNTs. For the former, the FTIR spectra exhibited a straight line and an absorbance peak was not assigned, indicating no surface modification. For the MWCNTs-COOH spectra, an absorption peak at 1,600  $\text{cm}^{-1}$  could be assigned to

the COOH group and a peak at 3,300  $\text{cm}^{-1}$  could be assigned to the OH group. These peaks are indicative of successful COOH modification. For the MWCNTs-PEG spectra, the 2,920  $\text{cm}^{-1}$  peak could be assigned to the methylene groups and the 1,100  $\text{cm}^{-1}$  peak to the C–O–C vibration. The absorbance bands at 1,570, 1,450, 1,400, and 1,240  $\text{cm}^{-1}$  are consistent with PEG absorbance, strongly suggesting the existence of PEG MWCNTs. The absorbance at 1,730  $\text{cm}^{-1}$  is typically associated with ester groups and indicates a chemical linkage between MWCNTs and PEG segments.

### X-ray photoelectron spectroscopy (XPS)

The XPS of functionalized MWCNTs were recorded to confirm the linkage between MWCNTs and grafted groups (Figure S2). The scan of functionalized MWCNTs showed the presence of carbon and oxygen. Except for pristine MWCNTs, the COOH and PEG derivatives had an oxygen atom peak with a binding energy of 532.5 eV.

### Thermogravimetric analysis (TGA)

TGA is used to monitor how changes in manufacturing conditions affect the percentage of carbon nanotubes within a sample. In the heating of up to 500°C, pristine MWCNTs lost ~ 1.3% of total weight (Figure S3). MWCNTs-PEG and MWCNTs-COOH lost 19.4% and 18.5% weight, respectively. Therefore, ~ 20 wt% of side groups were grafted onto MWCNTs, indicating the difference in properties between pristine and modified MWCNTs arose from these side moieties.

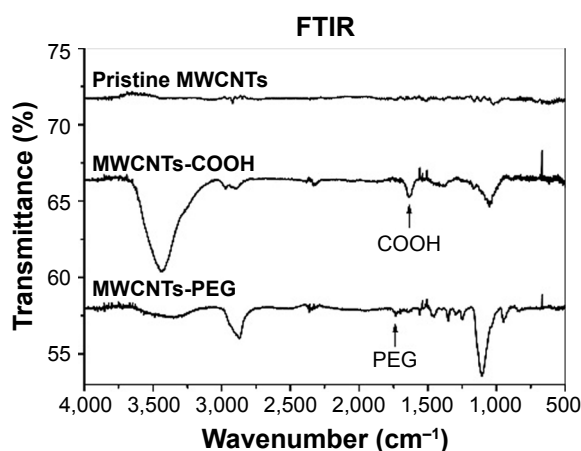


**Figure S1** FTIR spectra of MWCNTs in reflectance mode.

**Abbreviations:** FTIR, Fourier transform infrared spectroscopy; MWCNTs, multiwalled carbon nanotubes; MWCNTs-COOH, carboxylated MWCNTs; MWCNTs-PEG, polyethylene glycol MWCNTs.



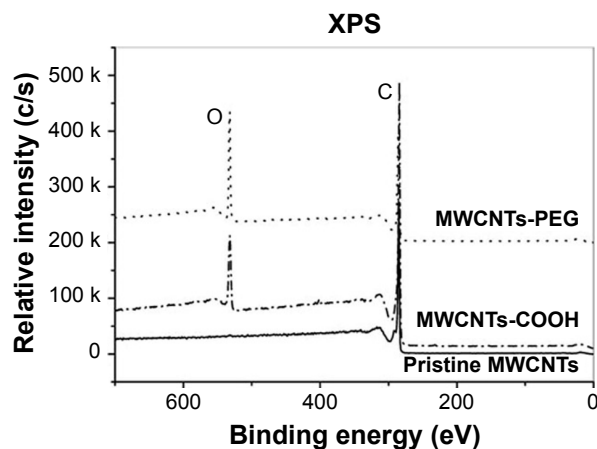


**Figure S2** C1s spectrum of MWCNTs, analyzed with X-ray photoelectron spectroscopy.

**Abbreviations:** MWCNTs, multiwalled carbon nanotubes; MWCNTs-COOH, carboxylated MWCNTs; MWCNTs-PEG, polyethylene glycol MWCNTs; XPS, X-ray photoelectron spectroscopy.

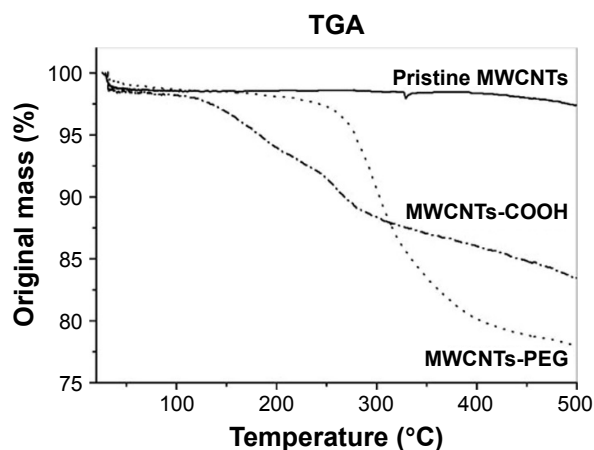


**Figure S3** TGA curves of MWCNTs in nitrogen atmosphere.

**Abbreviations:** MWCNTs, multiwalled carbon nanotubes; MWCNTs-COOH, carboxylated MWCNTs; MWCNTs-PEG, polyethylene glycol MWCNTs; TGA, thermal gravimetric analysis.

International Journal of Nanomedicine

Publish your work in this journal

The International Journal of Nanomedicine is an international, peer-reviewed journal focusing on the application of nanotechnology in diagnostics, therapeutics, and drug delivery systems throughout the biomedical field. This journal is indexed on PubMed Central, MedLine, CAS, SciSearch®, Current Contents®/Clinical Medicine,

Submit your manuscript here: <http://www.dovepress.com/international-journal-of-nanomedicine-journal>

Dovepress

Journal Citation Reports/Science Edition, EMBase, Scopus and the Elsevier Bibliographic databases. The manuscript management system is completely online and includes a very quick and fair peer-review system, which is all easy to use. Visit <http://www.dovepress.com/testimonials.php> to read real quotes from published authors.